UCLA
UCLA Previously Published Works

Title

CardioGPT: An ECG Interpretation Generation Model

Permalink

https://escholarship.org/uc/item/1gg179gn

Authors

Fu, Guohua

Zheng, Jianwei

Abudayyeh, Islam

et al.

Publication Date

2024

DOI

10.1109/access.2024.3384349

Peer reviewed

RESEARCH ARTICLE

CardioGPT: An ECG Interpretation Generation Model

GUOHUA FU[1,2], JIANWEI ZHENG[3], ISLAM ABUDAYYEH[3], CHIZOBAM ANI[3,4], CYRIL RAKOVSKI[5], LOUIS EHWERHEMUEPHA[6], HONGXIA LU[7], YONGJUAN GUO[2], SHENGLIN LIU[1], HUIMIN CHU[2], AND BING YANG[1]

[1]School of Medicine, Tongji University, Shanghai 200120, China
[2]The First Affiliated Hospital of Ningbo University, Ningbo, Zhejiang 315010, China
[3]Charles R. Drew University of Medicine and Science, Los Angeles, CA 90059, USA
[4]University of California at Los Angeles, Los Angeles, CA 90024, USA
[5]Schmid College of Science and Technology, Chapman University, Orange, CA 92886, USA
[6]Children's Hospital of Orange County, Orange, CA 92868, USA
[7]School of Medicine, University of North Carolina at Chapel Hill, Chapel Hill, NC 27599, USA

Corresponding author: Bing Yang (bingyang@tongji.edu.cn)

ABSTRACT Numerous supervised learning models aimed at classifying 12-lead electrocardiograms into different groups have shown impressive performance by utilizing deep learning algorithms. However, few studies are dedicated to applying the Generative Pre-trained Transformer (GPT) model in interpreting electrocardiogram (ECG) using natural language. Thus, we are pioneering the exploration of this uncharted territory by employing the CardioGPT model to tackle this challenge. We used a dataset of ECGs (standard 10s, 12-channel format) from adult patients, with 60 distinct rhythms or conduction abnormalities annotated by board-certified, actively practicing cardiologists. The ECGs were collected from The First Affiliated Hospital of Ningbo University and Shanghai East Hospital. The dataset is partitioned into training (80%), validation (10%), and test (10%) cohorts for comprehensive evaluation. Each cohort contains ECGs from distinct patients, considering some patients took repeated ECG measurements. The proposed algorithm is evaluated in two levels, self-performance measurement and comparison with the residual neural network classification model. Two scores are used for self-performance measurement, including Bilingual Evaluation Understudy (BLEU) and Recall-Oriented Understudy for Gisting Evaluation (ROUGE). To compare the performance of the proposed model with the residual neural network model, we assessed the F1 score and area under the receiver operating characteristic curve (AUC). We have observed promising performance metrics across multiple evaluation criteria through an extensive evaluation of a large 12-lead ECG database comprising 1,128,553 ECG readings from 754,920 patients. The CardioGPT model exhibited high BLEU and ROUGE scores with 0.68 (95% CI: 0.66, 0.71) and 0.81 (95% CI: 0.79, 0.84). Furthermore, in the classification performance measurement setting, the CardioGPT achieved an average F1-score of 0.91(95% CI: 0.89, 0.93) and AUC of 0.82(95% CI: 0.79, 0.84) and has higher scores than that of the convolutional neural network model, indicating its proficiency in accurately classifying ECG recordings. By leveraging the power of transformer structure model and natural language processing, the GPT model addresses the challenge of imbalanced learning commonly encountered in ECG classification tasks. The results indicate that the GPT model can accurately interpret ECG using natural language, providing valuable insights into the underlying patterns and abnormalities present in the data. Significance: The pioneering application of the GPT model for interpreting ECGs with natural language demonstrates its potential to address ECG classification challenges and offer valuable insights into cardiac health.

The associate editor coordinating the review of this manuscript and approving it for publication was Wai-Keung Fung .

I. INTRODUCTION

Heart disease is the leading cause of death globally, and standard 12 lead electrocardiogram (ECG) testing is an effective and economical tool in heart disease diagnostics, which can provide valuable information about the electrical activity of the heart [1]. The interpretation of ECG reading generally includes rhythms, conduction conditions, and abnormal morphological findings [2]. The interpretation of ECG signals is a challenging task that requires extensive training and expertise since multiple risky medical conditions can present avaricious ECG morphological representations [3]. Therefore, developing an automated ECG interpretation system can significantly benefit the medical community. Significant efforts have been made to develop an automated method for ECG classification, particularly for 12-lead ECGs, that mimics the accuracy of a human expert [4], [5]. Various approaches to achieving automatic ECG classification, including rule-based systems, template matching, and machine learning.

Rule-based systems use a set of predefined rules and algorithms to identify specific features and patterns in the ECG signal [6], [7]. The rules can be based on existing medical knowledge, making the interpretation consistent and reliable. This approach may not be flexible enough to handle all possible variations in ECG signals and may not be able to account for abnormalities with acceptable sensitivity and specificity. Template matching compares the ECG signal to a pre-existing database of templates to identify abnormalities [8], [9]. This approach shared similar pros and cons with rule-based methods. Machine learning algorithms use a large dataset of labeled ECG signals to train a model to identify patterns and classify the ECG signal into different categories [10], [11], [12], [13], [14]. Transformer neural network algorithms have been used to enhance model performance in ECG classification tasks [15], [16], [17] and time series data analysis [18]. These approaches have the potential to learn from large datasets and identify subtle patterns that may not be apparent to humans, leading to improved accuracy. They also require a large amount of high-quality data to train the algorithm and may be limited by the quality and representativeness of the data available. Additionally, these algorithms may be more difficult to interpret and explain, potentially leading to concerns about transparency and accountability.

All of the aforementioned methods simplified the issue by approaching ECG interpretations as a multilabel or multiclass classification problem. Consequently, they fail to incorporate the expertise of human professionals in diagnosing medical conditions or identifying ECG morphological abnormalities. In this study, we introduce a novel model, CardioGPT, designed to produce a natural language interpretation of ECGs, akin to the output of a human expert—an innovation unprecedented in its field. The CardioGPT model is trained on a large corpus of over a million ECGs from a diverse patient population. This proposed approach also employs a wavelet scattering network [19] for feature extraction, which can effectively capture complex patterns in ECG signals. Recent research works have shown the effectiveness of the wavelet scattering network as a feature extraction tool on ECG signals [20], [21], [22]. The wavelet scattering network is an enhancement over the conventional wavelet transform. Its advantages stem from its ability to offer both temporal and frequency resolutions that remain invariant to translations and stable against deformations, while preserving high-frequency information [19]. We then compare performance and saliency maps to baseline models subject to similar constraints. This research aims to develop a robust and accurate system for automatic ECG diagnosis in natural language, with potential implications for supporting healthcare professionals in identifying cardiac conditions.

II. METHODS
A. STUDY DESIGN

The study design, depicted in Fig. 1, provides an overview of the research approach. The dataset comprises 12 lead ECG waveform recordings and their corresponding textual diagnosis or explanations, where each recording is accompanied by one or more sentences offering interpretations from certified physicians. To enhance data quality, noise reduction techniques are applied to the ECG waveform recordings before utilizing the Wavelet Scattering Transformation to generate 3D wavelet scattering transformation feature matrices. To facilitate model training, the textual diagnosis is translated from Chinese to English using an OpenAI GPT-3 model [23], and subsequently, a GPT-4 completion model decomposes the textual diagnosis into classification labels. To prepare the data for further analysis, input data is preprocessed and flattened as required by subsequent models. The entire dataset is then divided into three cohorts: a training cohort (70%), a validation cohort (10%), and a testing cohort (20%). The training cohort is utilized to learn patterns from the data, whereas the validation cohort is employed to fine-tune hyperparameters like learning rate, epoch number, and layer configurations to optimize model performance. Lastly, the testing cohort is used to evaluate the model's effectiveness and to compare its performance against residual net neural network models.

B. DATA COLLECTION AND PROCESSING

Our dataset comprised retrospective data from adult patients (aged ≥18 years) who had an ECG at three hospitals. The dataset included standard 10 seconds, 12-channel ECGs recorded at a sampling rate of 500 Hz using ECG machines from GE Healthcare and Philips Healthcare. The institutional review boards of The First Affiliated Hospital of Ningbo University and Shanghai East Hospital approved this study
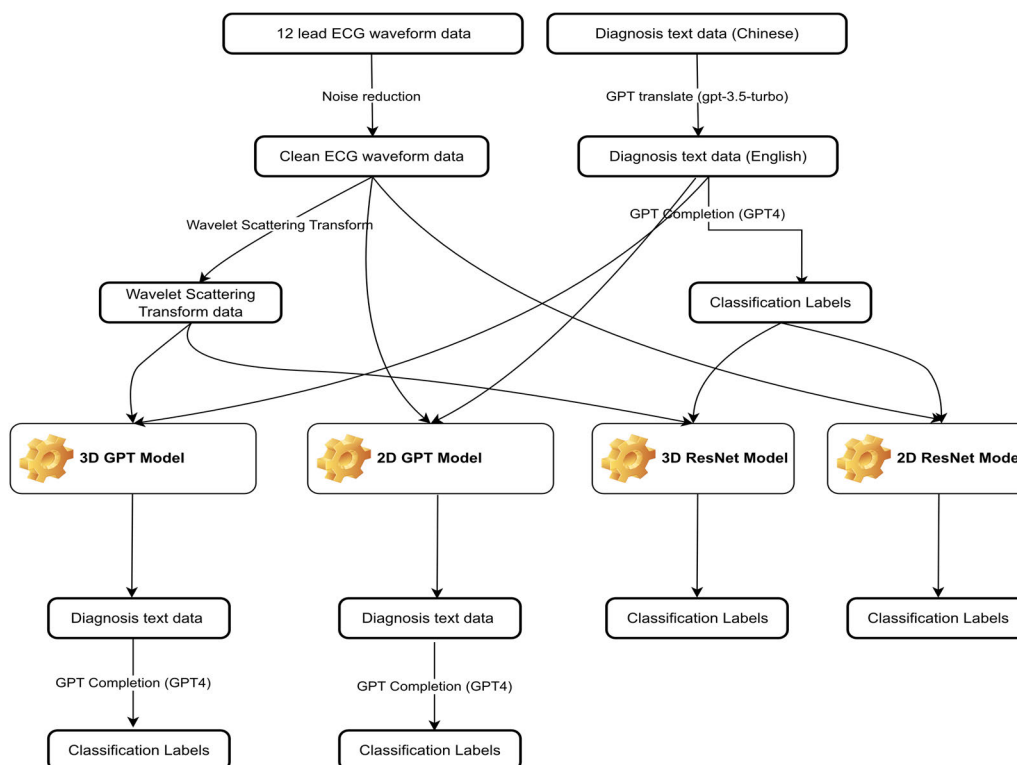
FIGURE 1. The overview of research approach and data flow in the study. The coefficients of wavelet scattering transformation are input of 3D GPT model and Resnet model. The 12 lead ECG waveform data are input for 2D models.

and granted the waiver application to obtain informed consent (approval code 2022RS036). The noise contamination sources in the ECG data were due to power line interference, electrode contact noise, motion artifacts, muscle contraction, baseline wandering, and random noise [24]. As is well known, the presence of noise can be a remarkable obstacle to any statistical analysis. Thus, we implemented a noise reduction approach to process raw ECG data. Since the frequency range of normal ECG is from 0.5Hz to 50Hz, the Butterworth bandpass filter [25] was used to remove the signal with a frequency above 50Hz and below 0.5 Hz. According to the standard ECG measurement mechanism [26], [27], two constraints must be satisfied: first, the voltage value of lead II should always be equal to the sum of voltage values of lead I and lead III; second, the sum of voltage values of lead aVR, aVL, and aVF should be equal to zero. Moreover, some of the electrodes could slip off during the test resulting in ECGs displaying a straight line. We created an automatic error-checking algorithm that detects the presence of these undesirable cases and excluded such ECG records from the study.

C. WAVELET SCATTERING NETWORK FOR FEATURE EXTRACTION

The wavelet scattering network [19], [28] is a type of deep neural network that can extract features from ECG signals

by decomposing them into a series of wavelet coefficients. The wavelet scattering network consists of a series of wavelet transforms and non-linear operations, which can capture complex patterns in ECG signals [29]. For example, Fig. 2. showcases the results of the Wavelet Scattering Transform applied to two ECG signals. Panel A displays a Lead II ECG signal representing Sinus Rhythm, while Panel B exhibits the corresponding ECG signal for Atrial Flutter. Upon applying the Wavelet Scattering Transform to the ECG signals, Panels C1 and C2 visualize the spectra of the wavelet-scattered ECG in Panel A (Sinus Rhythm). Similarly, Panels D1 and D2 depict the spectra of the wavelet-scattered ECG in Panel B (Atrial Flutter). The exceptional capability of the Wavelet Scattering Network accurately distinguished intricate distinctions in two types of ECG signals.

D. CARIDOGPT MODEL

The CardioGPT model represents a groundbreaking advancement in 12-lead ECG data interpretation, building upon the foundation of the Contrastive Language-Image Pretraining (CLIP) model developed by OpenAI [30]. CLIP, based on the GPT architecture, is a multimodal model renowned for its ability to comprehend both images and textual descriptions. By leveraging CLIP's powerful capabilities, we treat the 12-lead ECG data as a sequence of vectors, employing a transformer model comprising self- attention and
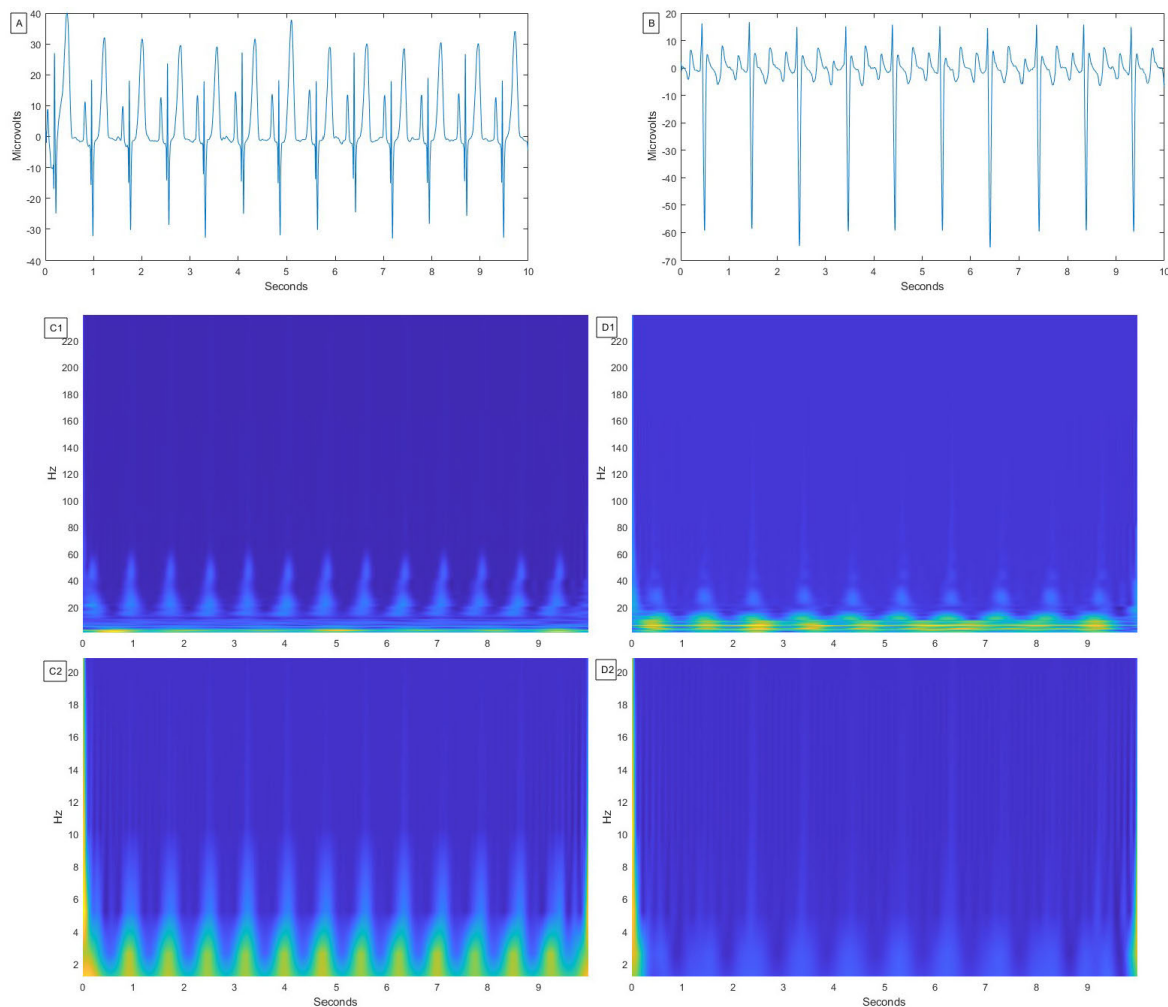
FIGURE 2. Wavelet scattering transform comparison for atrial flutter and sinus rhythm. Wavelet scattering transformation applied to lead II ECG data for two distinct cardiac rhythms: (A) Sinus rhythm and (B) Atrial flutter. Panels C1 and C2 display the spectra of the wavelet-scattered ECG in 2A, while panels D1 and D2 exhibit the spectra of the wavelet-scattered ECG in 2B.

feedforward layers that capture long-term dependencies in the input sequences.

To adapt the transformer model to handle 3D input variables and capture vital spatial information, additional architectural modifications and techniques are introduced. Here, we outline the primary steps involved in interpreting 3D input variables from Wavelet Scattering transformation using the CardioGPT model (shown in Fig. 3).

Patch Embedding (appendix 1 p 4): The input 3D feature is intelligently partitioned into smaller fixed-size (16 by 16) 2D patches, effectively converting them into tokens. These patches are then projected into lower-dimensional embeddings, enabling the model to capture essential local visual information.

Positional Encoding (appendix 1 p 4): To preserve the crucial spatial relationships between the patches, we incorporate positional encoding into the patch embeddings. This strategic addition provides each patch with a unique positional embedding, indicating its relative position within the image.

Consequently, the model gains a comprehensive understanding of the spatial layout of the patches.

Diagnosis Encoder: The diagnosis sentences undergo a tokenization encoder process, generating new representations in the form of a sequence of vectors. Each vector captures a specific component of the diagnosis sentence. The diagnosis vocabulary encompasses a total of 4157 distinct tokens, ensuring comprehensive coverage for accurate and meaningful representations.

E. STATISTICAL ANALYSIS

Two-sample t test, two-sample test for proportions, and Chi-square test were adopted to test the difference of the sample numbers, average ages, and genders between training and testing groups. The following performance measures were formally analyzed, including the receiver operating characteristic curve (AUC)and F1-score. A two-sided 95% CI summarizes the sample variability in the estimates. The CI for
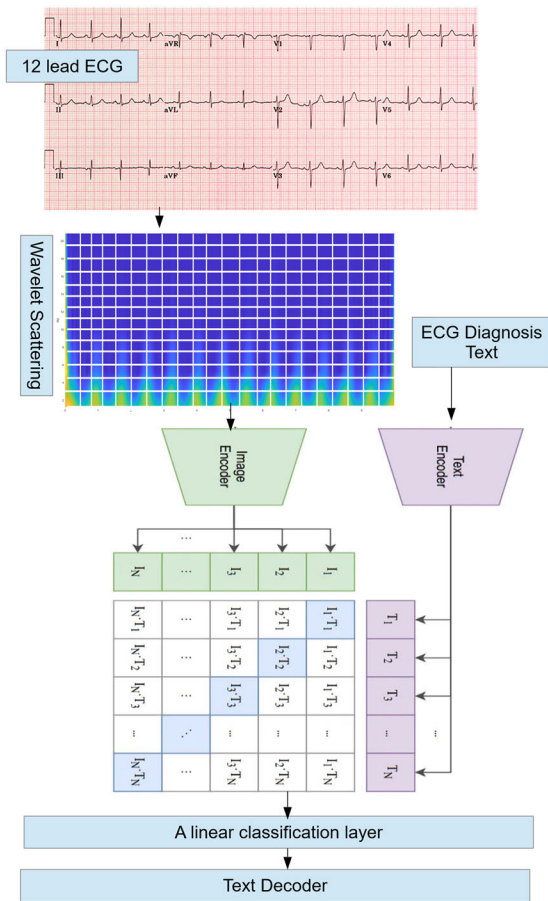
FIGURE 3. CardioGPT model architecture for 3D ECG data interpretation. The CardioGPT model integrates the foundational concepts of the Contrastive Language-Image Pretraining (CLIP) model to interpret 3D input variables from Wavelet Scattering transformations. The model employs patch embedding, positional encoding, and a diagnosis encoder to effectively capture spatial and diagnostic information, enabling comprehensive ECG data interpretation.

the AUC was estimated using the Sun and Su optimization of the Delong method implemented in the pROC package. In contrast, CIs for F1-score, and AUC were obtained by the bootstrap method with 20,000 replications. BLEU (Bilingual Evaluation Understudy) [31] is a commonly used metric that measures the similarity between the generated captions and reference captions (appendix 1 p 5). It calculates a score based on n-gram overlap between the generated and reference captions. Higher BLEU scores indicate better matching with reference captions. ROUGE (Recall-Oriented Understudy for Gisting Evaluation) [32] is a metric commonly used in text summarization tasks (appendix 1 p 6). It measures the overlap between the generated and reference captions based on n-grams. Higher ROUGE scores indicate better matching with reference captions. We use the package of NLTK to compute BLEU scores and the nlg-eval library to attain ROUGE scores. All analyses were done by R version 3.5.3 and Python 3.9.

III. RESULTS

The proposed approach is evaluated on a large ECG database with 1,128,553 ECG readings from 754,920 patients between Jan 1, 2013 and Dec 2022 (shown in Table 1). The database consists of 12 lead ECG waveforms and diagnoses text. Each diagnosis was used to generate 60 classification labels (shown in Table 1), which are designed for benchmark comparison with the convolutional neural network classification model. The mean age of the patients was 57.9 years (SD 15.8) and 32,377 (45.8%) were women. We validated our deep learning model with the test dataset consisting of 225,643 ECGs recorded, corresponding to 150,984 unique patients (89,080 [59%] women; mean age 50.8 years [SD 17.1]). 238,018 (26.36%) of the 902,910 ECGs in the training and validation dataset were multilabel, as were 59,730 (26.47%) of 225,643 in the test dataset (Fig. 4A). Fig 4B illustrates the distribution of ECGs with one label and more than one label among major rhythms. The major rhythms include sinus rhythm, sinus bradycardia, sinus tachycardia, sinus arrhythmia, atrial fibrillation, atrial flutter, and atrial tachycardia.

Table 2 presents the CardioGPT's performance using different feature inputs. Taking with 2D ECG data input, the CardioGPT achieves a BLEU score of 0.65 (with a 95% confidence interval of 0.62 to 0.78) and a ROUGE score of 0.78 (with a 95% confidence interval of 0.75 to 0.80). When using Wavelet Scattering Features with 3D input, the model's performance improves, achieving a higher BLEU score of 0.68 (with a 95% confidence interval of 0.66 to 0.71) and a higher ROUGE score of 0.81 (with a 95% confidence interval of 0.79 to 0.84).

Table 3 presents the F1-Score and AUC metrics for both the Transformer Model and the Residual Net Converlutional Neural Network (CNN) Model across 60 different cardiac conditions. The CardioGPT achieves an overall mean F1-Score of 0.91 (with a 95% confidence interval of 0.89 to 0.93) and an AUC of 0.82 (with a 95% confidence interval of 0.79 to 0.84). In comparison, the Residual Net CNN Model achieves a lower overall mean F1-Score of 0.83 (with a 95% confidence interval of 0.80 to 0.85) and an AUC ROC of 0.73 (with a 95% confidence interval of 0.69 to 0.75).

The results indicate that the Transformer Model outperforms the Residual Net CNN Model in terms of both F1-Score and AUC, suggesting that the Transformer Model is more effective in classifying various cardiac conditions.

IV. DISCUSSION

The accurate interpretation of ECG readings is paramount in guiding precise clinical decisions and timely interventions, underscoring its critical role in patient care [33]. ECGs offer essential insights into the presence, extent, and severity of arrhythmias such as atrial fibrillation, atrial flutter, supraventricular tachycardia, and atrioventricular block [34], [35]. However, physician interpretation of ECG readings is not without challenges. Notably, the precision of diagnosis might be compromised when distinguishing visually similar ECG waveforms or when dealing with combinations of multiple

TABLE 1. Baseline characteristics of the training, validation and testing cohorts. The data includes the number and percentage of individuals with specific electrocardiogram recordings, along with the mean age and standard deviation. P-values are provided to indicate significant differences between the two cohorts, and NA indicates not applicable.

	Training + Validation	Testing Cohort	P-Value
ECG recordings	902,910	225,643	NA
Age (mean±std)	53.56±18.91	49.5±18.39	<0.05
Male (n, %)	443,383 (49.11)	123,910 (54.91)	<0.05
Sinus rhythm (n, %)	651,846 (72.19)	162,961 (72.22)	0.80
Sinus bradycardia (n, %)	101,778 (11.27)	25,444 (11.28)	0.96
Sinus tachycardia (n, %)	47,555 (5.27)	11,889 (5.27)	0.97
High left ventricular voltage (n, %)	47,073 (5.21)	11,794 (5.23)	0.80
Sinus arrhythmia (n, %)	41,152 (4.56)	10,288 (4.56)	0.98
Atrial fibrillation (n, %)	37,042 (4.1)	9,261 (4.1)	0.97
Normal electrocardiogram (n, %)	32,561 (3.61)	8,140 (3.61)	0.98
Right axis deviation (n, %)	26,989 (2.99)	6,747 (2.99)	0.99
Left axis deviation (n, %)	26,734 (2.96)	6,683 (2.96)	0.99
Complete right bundle branch block (n, %)	25,215 (2.79)	6,325 (2.8)	0.79
Premature atrial contraction (n, %)	24,656 (2.73)	6,191 (2.74)	0.74
Premature ventricular contraction (n, %)	18,568 (2.06)	4,642 (2.06)	0.99
First degree atrioventricular block (n, %)	16,826 (1.86)	4,207 (1.86)	0.98
Incomplete right bundle branch block (n, %)	11,937 (1.32)	2,984 (1.32)	0.99
Early repolarization (n, %)	11,243 (1.25)	2,811 (1.25)	0.99
Poor data quality (n, %)	8,548 (0.95)	2,137 (0.95)	0.99
Left anterior fascicular block (n, %)	7,224 (0.8)	1,806 (0.8)	0.99
Clockwise rotation (n, %)	7,014 (0.78)	1,754 (0.78)	0.99
Counterclockwise rotation (n, %)	6,394 (0.71)	1,598 (0.71)	0.99
Atrial flutter (n, %)	5,299 (0.59)	1,325 (0.59)	0.99
Pacemaker rhythm (n, %)	4,058 (0.45)	1,015 (0.45)	0.99
Intraventricular conduction block (n, %)	4,651 (0.52)	1,190 (0.53)	0.48
Complete left bundle branch block (n, %)	4,373 (0.48)	1,096 (0.49)	0.95
Atrial tachycardia (n, %)	2,465 (0.27)	616 (0.27)	0.99
Atrial rhythm (n, %)	2,192 (0.24)	548 (0.24)	0.99
Supraventricular tachycardia (n, %)	2,163 (0.24)	541 (0.24)	0.99
Accelerated atrial rhythm (n, %)	2,104 (0.23)	526 (0.23)	0.99
No electrocardiographic activity seen (n, %)	1,932 (0.21)	483 (0.21)	0.99
Dual chamber pacemaker (n, %)	1,588 (0.18)	397 (0.18)	0.99
Acute anterior myocardial infarction (n, %)	1,371 (0.15)	347 (0.15)	0.86
Atrial paced rhythm (n, %)	1,187 (0.13)	297 (0.13)	0.99

TABLE 1. *(Continued.)* Baseline characteristics of the training, validation and testing cohorts. The data includes the number and percentage of individuals with specific electrocardiogram recordings, along with the mean age and standard deviation. P-values are provided to indicate significant differences between the two cohorts, and NA indicates not applicable.

First-degree atrioventricular block (n, %)	1,065 (0.12)	267 (0.12)	0.99
Atrioventricular conduction block (n, %)	884 (0.1)	221 (0.1)	0.99
Acute inferior myocardial infarction (n, %)	838 (0.09)	213 (0.09)	0.86
Junctional escape rhythm (n, %)	698 (0.08)	175 (0.08)	0.99
Acute coronary syndrome (n, %)	674 (0.07)	168 (0.07)	0.99
Second-degree atrioventricular block (n, %)	629 (0.07)	160 (0.07)	0.88
Junctional escape beat (n, %)	596 (0.07)	167 (0.07)	0.21
Atrial escape beat (n, %)	577 (0.06)	168 (0.07)	0.09
Ventricular pre-excitation (n, %)	529 (0.06)	132 (0.06)	0.99
Right ventricular hypertrophy (n, %)	498 (0.06)	125 (0.06)	0.99
Accelerated junctional rhythm (n, %)	483 (0.05)	121 (0.05)	0.99
Third-degree atrioventricular block (n, %)	478 (0.05)	120 (0.05)	0.99
Ventricular pre-excitation type B (n, %)	466 (0.05)	118 (0.05)	0.94
Right bundle branch block (n, %)	442 (0.05)	111 (0.05)	0.99
Sinus capture (n, %)	409 (0.05)	102 (0.05)	0.99
Ventricular tachycardia (n, %)	382 (0.04)	95 (0.04)	0.99
Ventricular conduction block (n, %)	354 (0.04)	93 (0.04)	0.71
Ventricular pre-excitation type A (n, %)	338 (0.04)	84 (0.04)	0.99
Complete atrioventricular dissociation (n, %)	324 (0.04)	88 (0.04)	0.53
Premature junctional contraction (n, %)	301 (0.03)	75 (0.03)	0.99
Atrial escape rhythm (n, %)	271 (0.03)	68 (0.03)	0.99
Ventricular escape beats (n, %)	264 (0.03)	69 (0.03)	0.79
Ventricular escape rhythm (n, %)	233 (0.03)	58 (0.03)	0.99
Sinus arrest (n, %)	179 (0.02)	47 (0.02)	0.83
Junctional rhythm (n, %)	180 (0.02)	45 (0.02)	0.99
Atrial arrhythmia (n, %)	131 (0.01)	33 (0.01)	0.99
Left bundle branch block (n, %)	104 (0.01)	30 (0.01)	0.56
Ventricular fibrillation (n, %)	102 (0.01)	26 (0.01)	0.99
Incomplete left bundle branch block (n, %)	83 (0.01)	24 (0.01)	0.61

conditions. Certain rhythm and conduction abnormalities, like sinus tachycardia, atrial tachycardia, idioventricular tachycardia, and ventricular tachycardia, exhibit subtle
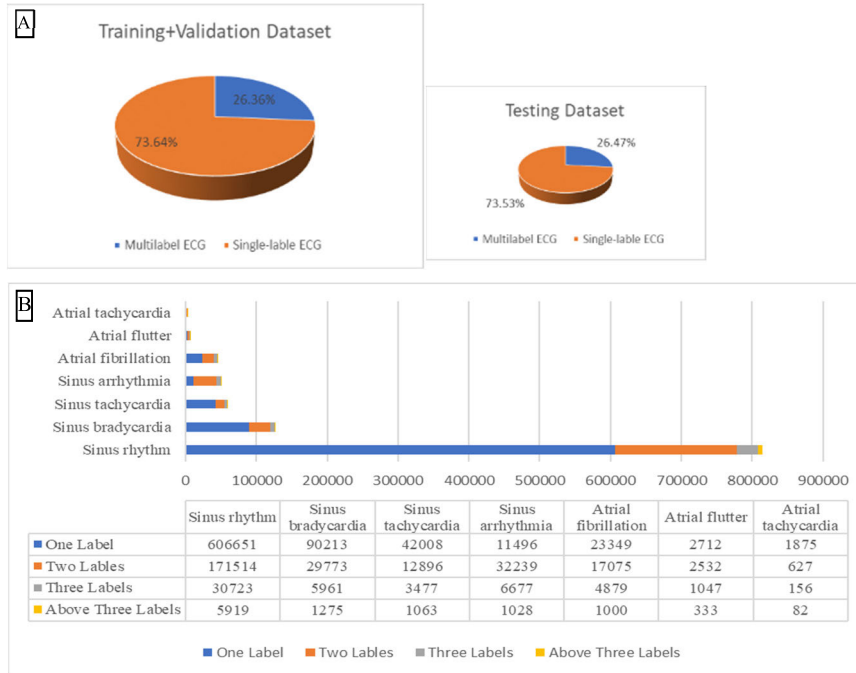
FIGURE 4. Analysis of multilabel ECG distribution and major rhythm classification. A shows the distribution of multilabel ECGs in the training, validation, and test datasets. B displays the distribution of ECGs categorized by major rhythms and the presence of one label or multiple labels.

TABLE 2. Model performance (95% CI) with different features input. The metrics of Bilingual Evaluation Understudy (BLEU) and Recall-Oriented Understudy for Gisting Evaluation (ROUGE) are reported, along with their respective 95% confidence intervals in parentheses. The results indicate the model's performance in generating outputs based on the different feature inputs.

	ECG data (2D)	Wavelet scattering Features (3D)
BLEU	0.65 (0.62, 0.78)	0.68 (0.66, 0.71)
ROUGE	0.78 (0.75, 0.8)	0.81 (0.79, 0.84)

differences in impulse origin sites, posing challenges, particularly for less experienced ECG interpreters [36].

Prior investigations in ECG interpretation predominantly utilized machine learning approaches that often focused on single or multilabel classification of ECG recordings [10], [11], [12], [13], [14]. However, they typically excluded expert estimations of medical conditions and ECG morphological abnormalities. Our study introduces a novel dimension by generating natural language interpretations of ECG readings, akin to those articulated by medical experts. Our CardioGPT model, combined with the wavelet scattering technique, excels in extracting comprehensive information from complete ECG diagnoses – a pivotal clinical endeavor. Impressively, the model attains BLEU and ROUGE scores of 0.68 (95%CI: 0.66, 0.71) and 0.81 (95%CI: 0.79, 0.84), respectively.

Harnessing the synergy of wavelet scattering networks and transformer models, our CardioGPT model was trained on an expansive dataset of 754,920 patients encompassing 59 types of abnormal ECGs and a normal counterpart. This dataset comprehensively represents rhythms, conduction abnormalities, and morphological findings. Notably, over 25% of ECG readings exhibit multiple condition labels, augmenting dataset complexity and encompassing a diverse array of abnormalities (Fig. 4). Our results establish CardioGPT's superiority, outperforming several existing methods in terms of AUC scores for multilabel ECG classification. This success owes to the wavelet scattering network's ability to capture intricate ECG signal patterns, facilitating the CardioGPT model in learning discriminative features for precise ECG interpretation. For instance, the diagnosis of atrial fibrillation attains a mean F1-score of 0.95 (95% CI: 0.90, 0.99), underscoring the algorithm's adeptness in extracting and discerning complex features even amidst highly similar ECG waveforms.

Additionally, our study's ECGs derive from diverse sources, encompassing two hospitals with distinct ECG machines and a large patient cohort spanning genders, ages, and various clinical heart conditions – including patients with multiple arrhythmias. This diversity augments the spectrum of diseases represented in our dataset. We also devised a robust comparison methodology with a mainstream Residual Neural Network model, highlighting our model's superior classification accuracies and F1 scores across different rhythm classes.

Remarkably, our work pioneers a deep learning approach that systematically investigates nearly all rhythm and conduction dysfunction-induced arrhythmias. The result is an end-to-end, AI-driven, automated ECG interpretation model,

TABLE 3. Comparison of classification performance between GPT and CNN models with 95% confidence intervals. The F1-score and AUC metrics are used to evaluate the models' performance for 60 different conditions, including sinus rhythm, sinus bradycardia, sinus tachycardia, high left ventricular voltage, sinus arrhythmia, atrial fibrillation etc. The values in parentheses represent the 95% confidence intervals for each performance metric.

Conditions	Transformer Model		Residual Net CNN Model	
	F1-Score	AUC	F1-Score	AUC
Sinus rhythm	0.95(0.90, 0.99)	0.84(0.80, 0.89)	0.80(0.75, 0.86)	0.89(0.84, 0.94)
Sinus bradycardia	0.99(0.92, 1.06)	0.88(0.84, 0.93)	0.84(0.79, 0.88)	0.86(0.81, 0.91)
Sinus tachycardia	0.97(0.90, 1.04)	0.82(0.78, 0.86)	0.82(0.75, 0.89)	0.83(0.79, 0.88)
High left ventricular voltage	0.96(0.90, 1.03)	0.92(0.88, 0.96)	0.80(0.74, 0.86)	0.81(0.76, 0.86)
Sinus arrhythmia	0.93(0.88, 0.98)	0.81(0.77, 0.85)	0.85(0.79, 0.92)	0.83(0.78, 0.88)
Atrial fibrillation	0.93(0.89, 0.97)	0.95(0.90, 0.99)	0.77(0.71, 0.84)	0.83(0.79, 0.87)
Normal electrocardiogram	0.92(0.86, 0.98)	0.92(0.87, 0.96)	0.80(0.74, 0.86)	0.87(0.82, 0.92)
Right axis deviation	0.98(0.93, 1.03)	0.83(0.78, 0.87)	0.81(0.74, 0.88)	0.86(0.82, 0.91)
Left axis deviation	0.96(0.92, 1.01)	0.80(0.75, 0.85)	0.83(0.78, 0.87)	0.89(0.84, 0.94)
Complete right bundle branch block	0.97(0.91, 1.02)	0.92(0.88, 0.96)	0.88(0.84, 0.93)	0.85(0.80, 0.90)
Premature atrial contraction	0.92(0.88, 0.96)	0.91(0.86, 0.95)	0.78(0.74, 0.83)	0.81(0.77, 0.86)
Premature ventricular contraction	0.99(0.92, 1.06)	0.91(0.86, 0.96)	0.84(0.79, 0.89)	0.87(0.83, 0.91)
First degree atrioventricular block	0.98(0.93, 1.03)	0.92(0.87, 0.96)	0.85(0.80, 0.90)	0.88(0.83, 0.92)
Incomplete right bundle branch block	0.93(0.87, 0.99)	0.81(0.77, 0.85)	0.76(0.71, 0.81)	0.86(0.81, 0.90)
Early repolarization	0.93(0.88, 0.98)	0.85(0.81, 0.90)	0.85(0.79, 0.92)	0.88(0.83, 0.93)
Poor data quality	0.93(0.88, 0.99)	0.82(0.78, 0.86)	0.78(0.73, 0.83)	0.85(0.80, 0.90)
Left anterior fascicular block	0.80(0.75, 0.85)	0.82(0.78, 0.87)	0.78(0.72, 0.83)	0.72(0.68, 0.77)
Clockwise rotation	0.86(0.80, 0.92)	0.85(0.80, 0.90)	0.76(0.69, 0.83)	0.74(0.69, 0.78)
Counterclockwise rotation	0.85(0.79, 0.91)	0.80(0.76, 0.85)	0.78(0.74, 0.83)	0.73(0.68, 0.78)
Atrial flutter	0.83(0.76, 0.89)	0.78(0.73, 0.83)	0.76(0.70, 0.81)	0.74(0.70, 0.79)
Pacemaker rhythm	0.81(0.75, 0.87)	0.83(0.78, 0.88)	0.78(0.72, 0.85)	0.74(0.70, 0.78)
Intraventricular conduction block	0.84(0.78, 0.90)	0.78(0.73, 0.82)	0.77(0.71, 0.83)	0.72(0.67, 0.77)
Complete left bundle branch block	0.91(0.87, 0.96)	0.79(0.75, 0.84)	0.80(0.74, 0.86)	0.71(0.67, 0.76)
Atrial tachycardia	0.84(0.79, 0.89)	0.76(0.71, 0.81)	0.76(0.70, 0.82)	0.74(0.69, 0.78)
Atrial rhythm	0.86(0.81, 0.91)	0.75(0.71, 0.79)	0.77(0.72, 0.82)	0.71(0.66, 0.76)
Supraventricular tachycardia	0.88(0.84, 0.93)	0.85(0.80, 0.90)	0.76(0.71, 0.80)	0.73(0.68, 0.78)
Accelerated atrial rhythm	0.84(0.77, 0.91)	0.83(0.79, 0.88)	0.80(0.73, 0.86)	0.75(0.70, 0.80)
No electrocardiographic activity seen	0.92(0.86, 0.97)	0.82(0.77, 0.87)	0.79(0.73, 0.86)	0.73(0.69, 0.78)
Dual chamber pacemaker	0.92(0.85, 0.98)	0.79(0.75, 0.83)	0.76(0.70, 0.83)	0.73(0.68, 0.77)
Acute anterior myocardial infarction	0.83(0.77, 0.89)	0.77(0.72, 0.82)	0.78(0.72, 0.85)	0.74(0.69, 0.78)
Atrial paced rhythm	0.86(0.80, 0.92)	0.77(0.72, 0.81)	0.79(0.74, 0.85)	0.73(0.68, 0.78)
First-degree atrioventricular block	0.84(0.78, 0.89)	0.78(0.73, 0.82)	0.78(0.72, 0.83)	0.73(0.69, 0.78)
Atrioventricular conduction block	0.83(0.78, 0.89)	0.80(0.76, 0.85)	0.78(0.71, 0.84)	0.75(0.70, 0.79)
Acute inferior myocardial infarction	0.80(0.75, 0.86)	0.82(0.78, 0.86)	0.76(0.70, 0.82)	0.73(0.68, 0.77)
Junctional escape rhythm	0.87(0.83, 0.92)	0.82(0.77, 0.86)	0.75(0.69, 0.82)	0.75(0.71, 0.79)
Acute Coronary Syndrome	0.86(0.80, 0.92)	0.78(0.73, 0.83)	0.79(0.73, 0.86)	0.75(0.70, 0.79)
Second-degree atrioventricular block	0.81(0.76, 0.85)	0.85(0.80, 0.89)	0.80(0.73, 0.86)	0.72(0.68, 0.76)
Junctional escape beat	0.83(0.79, 0.87)	0.82(0.78, 0.87)	0.78(0.73, 0.83)	0.71(0.67, 0.76)
Atrial escape beat	0.91(0.85, 0.97)	0.81(0.76, 0.85)	0.77(0.72, 0.82)	0.71(0.67, 0.75)
Ventricular pre-excitation	0.83(0.78, 0.87)	0.81(0.77, 0.86)	0.77(0.72, 0.81)	0.71(0.67, 0.75)
Right ventricular hypertrophy	0.82(0.75, 0.89)	0.79(0.75, 0.83)	0.79(0.73, 0.84)	0.71(0.67, 0.75)
Accelerated junctional rhythm	0.86(0.79, 0.93)	0.77(0.73, 0.82)	0.79(0.75, 0.84)	0.74(0.69, 0.78)
Third-degree atrioventricular block	0.92(0.85, 0.99)	0.79(0.74, 0.83)	0.79(0.74, 0.85)	0.71(0.67, 0.76)
Ventricular pre-excitation type B	0.83(0.78, 0.88)	0.83(0.78, 0.87)	0.79(0.73, 0.85)	0.72(0.68, 0.77)
Right bundle branch block	0.88(0.84, 0.92)	0.75(0.70, 0.80)	0.78(0.73, 0.83)	0.74(0.69, 0.79)
Sinus capture	0.89(0.82, 0.96)	0.76(0.71, 0.81)	0.75(0.70, 0.81)	0.71(0.67, 0.75)
Ventricular tachycardia	0.83(0.78, 0.88)	0.75(0.71, 0.80)	0.76(0.72, 0.80)	0.74(0.70, 0.79)
Ventricular conduction block	0.89(0.82, 0.96)	0.75(0.71, 0.80)	0.79(0.75, 0.84)	0.72(0.67, 0.77)
Ventricular pre-excitation type A	0.84(0.78, 0.91)	0.84(0.79, 0.88)	0.78(0.72, 0.84)	0.71(0.67, 0.76)
Complete atrioventricular dissociation	0.88(0.81, 0.94)	0.82(0.77, 0.87)	0.75(0.70, 0.80)	0.74(0.69, 0.79)
Premature junctional contraction	0.88(0.83, 0.92)	0.80(0.75, 0.84)	0.76(0.71, 0.80)	0.74(0.70, 0.78)
Atrial escape rhythm	0.86(0.81, 0.92)	0.76(0.71, 0.81)	0.78(0.73, 0.84)	0.75(0.70, 0.79)
Ventricular escape beats	0.81(0.75, 0.88)	0.80(0.76, 0.84)	0.75(0.69, 0.81)	0.74(0.70, 0.78)
Ventricular escape rhythm	0.90(0.85, 0.95)	0.80(0.76, 0.84)	0.76(0.71, 0.80)	0.74(0.69, 0.79)
Sinus arrest	0.84(0.79, 0.88)	0.77(0.73, 0.81)	0.78(0.72, 0.84)	0.72(0.68, 0.77)
Junctional rhythm	0.82(0.77, 0.88)	0.79(0.75, 0.84)	0.78(0.74, 0.83)	0.72(0.67, 0.77)
Atrial arrhythmia	0.80(0.74, 0.87)	0.79(0.74, 0.84)	0.78(0.74, 0.82)	0.74(0.70, 0.78)
Left bundle branch block	0.87(0.81, 0.93)	0.81(0.77, 0.85)	0.76(0.71, 0.82)	0.74(0.70, 0.79)
Ventricular fibrillation	0.88(0.82, 0.94)	0.81(0.77, 0.85)	0.79(0.73, 0.84)	0.75(0.70, 0.80)
Incomplete left bundle branch block	0.80(0.76, 0.84)	0.75(0.71, 0.80)	0.76(0.70, 0.82)	0.73(0.68, 0.77)
Mean	0.91(0.89, 0.93)	0.82(.79, 0.84)	0.83(0.8, 0.85)	0.73(0.69, 0.75)

signifying an unprecedented advance. This study underscores the significance of advanced wavelet scattering features and the CardioGPT model in precise ECG analysis, offering robust outputs and accurate cardiac condition classification. By amalgamating CLIP's strengths with tailored transformer model adaptations, CardioGPT emerges as a leading-edge solution for 12-lead ECG data interpretation. Its unique prowess in comprehending both images and text, coupled with its adept handling of 3D input variables, ushers in novel avenues for advanced diagnostics and analysis in cardiology. These findings portend enhanced automated ECG interpretation systems, fostering improved patient outcomes and contributing to streamlined, dependable cardiac diagnoses.

V. STUDY LIMITATIONS

While our study presents a promising approach for ECG interpretation using the CardioGPT model, it is essential to acknowledge the following limitations. Our evaluation is based on a large ECG database with 754,920 patients. However, the data in this database might be subject to certain biases, such as the demographics of the patient population, data collection procedures, and the quality of annotations. These biases could potentially impact the generalizability of our model to diverse patient populations or real-world clinical settings. Secondly, the proposed approach utilizes both wavelet scattering networks and transformer models, which can be computationally intensive, especially for large and complex ECG signals with multiple leads. Deploying the CardioGPT model in real-time clinical applications might require careful consideration of computational resources and optimization strategies. Finally, although our approach yields superior performance, the interpretability of the model's decisions could be a challenge. Deep learning models, including transformers, are known for their black-box nature, making it difficult to provide transparent explanations for the model's predictions. Ensuring the interpretability of the CardioGPT model is an ongoing area of research.

APPENDIX

Appendix is available online.

DATA AND CODE AVAILABILITY

While we are unable to share the full dataset due to privacy or proprietary constraints, we are committed to sharing a portion of the dataset used in our study. This partial dataset, representative of the overall dataset used in our experiments, is made available in a publicly accessible repository (PhysioNet. https://doi.org/10.13026/wgex-er52.). The MATALB program for ECG denoising was put under https://github.com/zheng120/ECGDenoisingTool.

ACKNOWLEDGMENT

This study received significant support from the ECG departments of The First Affiliated Hospital of Ningbo University and Shanghai East Hospital.

DECLARATION OF COMPETING INTEREST

The authors declare that they have no known competing financial interests or personal relationships that could have appeared to influence the work reported in this article.

REFERENCES

[1] "Heart rate variability: Standards of measurement, physiological interpretation and clinical use. Task force of the European Society of Cardiology and the North American Society of Pacing and Electrophysiology," *Circulation*, vol. 93, no. 5, pp. 1043–1065, Mar. 1996.

[2] R. C. Schlant, R. J. Adolph, J. P. DiMarco, L. S. Dreifus, M. I. Dunn, C. Fisch, A. Garson, L. J. Haywood, H. J. Levine, and J. A. Murray, "Guidelines for electrocardiography. A report of the American College of Cardiology/American Heart Association task force on assessment of diagnostic and therapeutic cardiovascular procedures (Committee on Electrocardiography)," *Circulation*, vol. 85, no. 3, pp. 1221–1228, Mar. 1992, doi: 10.1161/01.cir.85.3.1221.

[3] H. Holst, M. Ohlsson, C. Peterson, and L. Edenbrandt, "A confident decision support system for interpreting electrocardiograms," *Clin. Physiol.*, vol. 19, no. 5, pp. 410–418, Oct. 1999, doi: 10.1046/j.1365-2281.1999.00195.x.

[4] N. Maglaveras, T. Stamkopoulos, K. Diamantaras, C. Pappas, and M. Strintzis, "ECG pattern recognition and classification using non-linear transformations and neural networks: A review," *Int. J. Med. Informat.*, vol. 52, nos. 1–3, pp. 191–208, Oct. 1998, doi: 10.1016/s1386-5056(98)00138-5.

[5] S. W. Chen, S. L. Wang, X. Z. Qi, S. M. Samuri, and C. Yang, "Review of ECG detection and classification based on deep learning: Coherent taxonomy, motivation, open challenges and recommendations," *Biomed. Signal Process. Control*, vol. 74, Apr. 2022, Art. no. 103493, doi: 10.1016/j.bspc.2022.103493.

[6] M. Al-Ani and A. Ayal, "A rule-based expert system for automated ECG diagnosis," *Int. J. Adv. Eng. Technol.*, vol. 6, no. 4, pp. 1480–1493, 2013.

[7] K. P. Birman, "Rule-based learning for more accurate ECG analysis," *IEEE Trans. Pattern Anal. Mach. Intell.*, vols. PAMI–4, no. 4, pp. 369–380, Jul. 1982, doi: 10.1109/TPAMI.1982.4767268.

[8] G. Bansal, P. Gera, and D. R. Bathula, "Template based classification of cardiac arrhythmia in ECG data," in *Proc. IEEE 2nd Int. Conf. Recent Trends Inf. Syst. (ReTIS)*, Jul. 2015, pp. 337–341, doi: 10.1109/RETIS.2015.7232901.

[9] Q. Zhou, Y. Lu, and H. Duan, "Notice of retraction: ECG beat classification based on mirrored Gauss model and cluster template," in *Proc. 1st Int. Conf. Bioinf. Biomed. Eng.*, Jul. 2007, pp. 675–678, doi: 10.1109/ICBBE.2007.176.

[10] A. Y. Hannun, P. Rajpurkar, M. Haghpanahi, G. H. Tison, C. Bourn, M. P. Turakhia, and A. Y. Ng, "Cardiologist-level arrhythmia detection and classification in ambulatory electrocardiograms using a deep neural network," *Nature Med.*, vol. 25, no. 1, pp. 65–69, Jan. 2019, doi: 10.1038/s41591-018-0268-3.

[11] Z. I. Attia, S. Kapa, X. Yao, F. Lopez-Jimenez, T. L. Mohan, P. A. Pellikka, R. E. Carter, N. D. Shah, P. A. Friedman, and P. A. Noseworthy, "Prospective validation of a deep learning electrocardiogram algorithm for the detection of left ventricular systolic dysfunction," *J. Cardiovascular Electrophysiol.*, vol. 30, no. 5, pp. 668–674, May 2019.

[12] J. Zhang, S. Gajjala, P. Agrawal, G. H. Tison, L. A. Hallock, L. Beussink-Nelson, M. H. Lassen, E. Fan, M. A. Aras, C. Jordan, K. E. Fleischmann, M. Melisko, A. Qasim, S. J. Shah, R. Bajcsy and R. C. Deo, "Fully automated echocardiogram interpretation in clinical practice: Feasibility and diagnostic accuracy," *Circulation*, vol. 138, no. 16, pp. 1623–1635, 2018.

[13] Z. Ebrahimi, M. Loni, M. Daneshtalab, and A. Gharehbaghi, "A review on deep learning methods for ECG arrhythmia classification," *Expert Syst. Appl.*, vol. 7, Sep. 2020, Art. no. 100033, doi: 10.1016/j.eswax.2020.100033.

[14] H. Zhu, C. Cheng, H. Yin, X. Li, P. Zuo, J. Ding, F. Lin, J. Wang, B. Zhou, Y. Li, S. Hu, Y. Xiong, B. Wang, G. Wan, X. Yang, and Y. Yuan, "Automatic multilabel electrocardiogram diagnosis of heart rhythm or conduction abnormalities with deep learning: A cohort study," *Lancet Digit. Health*, vol. 2, no. 7, pp. e348–e357, Jul. 2020.

[15] C. Ji, L. Wang, J. Qin, L. Liu, Y. Han, and Z. Wang, "MSGformer: A multi-scale grid transformer network for 12-lead ECG arrhythmia detection," *Biomed. Signal Process. Control*, vol. 87, Jan. 2024, Art. no. 105499, doi: 10.1016/j.bspc.2023.105499.

[16] X. Xie, H. Liu, D. Chen, M. Shu, and Y. Wang, "Multilabel 12-lead ECG classification based on leadwise grouping multibranch network," *IEEE Trans. Instrum. Meas.*, vol. 71, pp. 1–11, 2022, doi: 10.1109/TIM.2022.3164141.

[17] R. Cheng, Z. Zhuang, S. Zhuang, L. Xie, and J. Guo, "MSW-Transformer: Multi-scale shifted windows transformer networks for 12-lead ECG classification," 2023, *arXiv:2306.12098*.

[18] Y. Jiang, Z. Pan, X. Zhang, S. Garg, A. Schneider, Y. Nevmyvaka, and D. Song, "Empowering time series analysis with large language models: A survey," 2024, *arXiv:2402.03182*.

[19] J. Bruna and S. Mallat, "Invariant scattering convolution networks," *IEEE Trans. Pattern Anal. Mach. Intell.*, vol. 35, no. 8, pp. 1872–1886, Aug. 2013, doi: 10.1109/TPAMI.2012.230.

[20] A. Sepúlveda, F. Castillo, C. Palma, and M. Rodriguez-Fernandez, "Emotion recognition from ECG signals using wavelet scattering and machine learning," *Appl. Sci.*, vol. 11, no. 11, p. 4945, May 2021.

[21] F. Liu, S. Xia, S. Wei, L. Chen, Y. Ren, X. Ren, Z. Xu, S. Ai, and C. Liu, "Wearable electrocardiogram quality assessment using wavelet scattering and LSTM," *Frontiers Physiol.*, vol. 13, Jun. 2022, Art. no. 905447.

[22] S. Nahak, A. Pathak, and G. Saha, "Fragment-level classification of ECG arrhythmia using wavelet scattering transform," *Expert Syst. Appl.*, vol. 224, Aug. 2023, Art. no. 120019.

[23] T. B. Brown et al., "Language models are few-shot learners," in *Proc. Adv. Neural Inf. Process. Syst.*, 2020, pp. 1877–1901.

[24] N. Kannathal, U. R. Acharya, K. P. Joseph, L. C. Min, and J. S. Suri, "Analysis of electrocardiograms," in *Advances in Cardiac Signal Processing*, 2007, pp. 55–82.

[25] S. Butterworth, "On the theory of filter amplifiers," *Exp. Wireless Wireless Eng.*, vol. 7, pp. 536–541, Oct. 1930.

[26] J. Zheng, J. Zhang, S. Danioko, H. Yao, H. Guo, and C. Rakovski, "A 12-lead electrocardiogram database for arrhythmia research covering more than 10,000 patients," *Sci. Data*, vol. 7, no. 1, p. 48, Feb. 2020, doi: 10.1038/s41597-020-0386-x.

[27] J. Zheng, H. Chu, D. Struppa, J. Zhang, S. M. Yacoub, H. El-Askary, A. Chang, L. Ehwerhemuepha, I. Abudayyeh, A. Barrett, G. Fu, H. Yao, D. Li, H. Guo, and C. Rakovski, "Optimal multi-stage arrhythmia classification approach," *Sci. Rep.*, vol. 10, no. 1, p. 2898, Feb. 2020, doi: 10.1038/s41598-020-59821-7.

[28] S. Mallat, "Group invariant scattering," *Commun. Pure Appl. Math.*, vol. 65, no. 10, pp. 1331–1398, Oct. 2012, doi: 10.1002/cpa.21413.

[29] J. Zheng, I. Abudayyeh, G. Mladenov, D. Struppa, G. Fu, H. Chu, and C. Rakovski, "An artificial intelligence-based noninvasive solution to estimate pulmonary artery pressure," *Frontiers Cardiovascular Med.*, vol. 9, Aug. 2022.

[30] A. Radford, J. W. Kim, C. Hallacy, A. Ramesh, G. Goh, S. Agarwal, G. Sastry, A. Askell, P. Mishkin, J. Clark, G. Krueger, and I. Sutskever, "Learning transferable visual models from natural language supervision," in *Proc. Int. Conf. Mach. Learn.*, 2021, pp. 8748–8763.

[31] M. Post, "A call for clarity in reporting BLEU scores," 2018, *arXiv:1804.08771*.

[32] C.-Y. Lin, "ROUGE: A package for automatic evaluation of summaries," in *Text Summarization Branches Out*, 2004, pp. 74–81.

[33] P. J. Kannankeril and F. A. Fish, "Management of common arrhythmias and conduction abnormalities," *Prog. Pediatric Cardiol.*, vol. 17, no. 1, pp. 41–52, Jul. 2003, doi: 10.1016/s1058-9813(03)00014-6.

[34] B. Surawicz, R. Childers, B. J. Deal, and L. S. Gettes, "AHA/ACCF/HRS recommendations for the standardization and interpretation of the electrocardiogram," *Circulation*, vol. 119, no. 10, pp. 235–240, Mar. 2009, doi: 10.1161/circulationaha.108.191095.

[35] V. Fuster et al., "ACC/AHA/ESC guidelines for the management of patients with atrial fibrillation: Executive summary. A report of the American College of Cardiology/American Heart Association task force on practice guidelines and the European Society of Cardiology Committee for Practice Guidelines and Policy Conferences (committee to develop guidelines for the management of patients with atrial fibrillation): Developed in collaboration with the North American Society of Pacing and Electrophysiology," *J. Amer. College Cardiol.*, vol. 38, no. 4, pp. 1231–1265, Oct. 2001, doi: 10.1016/s0735-1097(01)01587-x.

[36] W. Bonney, "Atrioventricular conduction abnormalities: Preexcitation, heart block, and other ventricular conduction abnormalities," in *Pediatric Electrocardiography: An Algorithmic Approach To Interpretation*, R.-I. Abdulla, W. Bonney, O. Khalid, and S. Awad, Eds. Cham, Switzerland: Springer, 2016, pp. 61–73.

GUOHUA FU received the master's degree in internal medicine with a specialization in cardiovascular medicine from Southern Medical University, in June 2013, and the Ph.D. degree in internal medicine from the School of Medicine, Tongji University, in July 2019.

She is a distinguished Cardiologist with a rich academic background and extensive clinical expertise. Since July 2013, she has been contributing significantly to the field of cardiology, holding a prominent position with the Cardiovascular Department, The Affiliated First Hospital of Ningbo University. Her dedication and proficiency in the diagnosis and treatment of various cardiac arrhythmias, including paroxysmal supraventricular tachycardia, atrial fibrillation, atrial flutter, atrial tachycardia, atrial premature contractions, and ventricular premature contractions, have established her as a leading expert in the field. Her clinical expertise extends beyond arrhythmias, as she specializes in the diagnosis and management of hypertension, coronary artery disease, and heart failure. Her commitment to advancing cardiovascular medicine is evident through her active involvement in cutting-edge research and her role in providing high-quality patient care. She continues to be a driving force in the field of cardiology, blending her clinical acumen with academic rigor to make lasting contributions to the understanding and treatment of cardiovascular diseases.
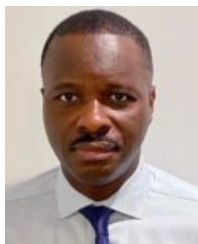
JIANWEI ZHENG received the Ph.D. degree in computational and data sciences from Chapman University, in 2021. His research interest includes the application of machine learning to ECG analysis for cardiovascular disease.

ISLAM ABUDAYYEH is a distinguished Medical Professional with a comprehensive academic background and extensive expertise in hemodynamics and biologic sciences, particularly in cardiovascular and structural heart diseases. Currently, he is a Professor of medicine with Loma Linda University, Loma Linda Veterans Administration Healthcare; and an Associate Professor of medicine with Charles R. Drew University of Medicine and Science and the University of California at Irvine. He has made significant contributions to the field of medicine.

CHIZOBAM ANI received the degree from the University College Hospital, Ibadan, Nigeria, the M.P.H. degree from Wichita State University and the University of Kansas, and the Ph.D. degree in epidemiology from Loma Linda University. He completed his residency training in internal medicine from Loma Linda University. He is an Internist and an Epidemiologist. He is currently working on several studies aimed at understanding the unique role of diabetes on cardiomyopathy and heart failure. He has been an investigator on several federally funded research grants and authored or coauthored several peer-reviewed research articles and a book chapter. His primary research interest is focused on cardiometabolic diseases, particularly risk factors and interventions to mitigate these risks among minority ethnic communities.

CYRIL RAKOVSKI received the Ph.D. degree in biostatistics from Harvard University, in 2006. He was a Postdoctoral Research Fellow with USC, from 2006 to 2008. Then, he joined Chapman University, where he is currently an Associate Professor. His research interests include the genetics analysis, time series data analysis, machine learning, and statistical modeling.

LOUIS EHWERHEMUEPHA is the Manager of the Research Computational Science (Computational Research) Team, CHOC under the executive leadership of Phuong Dao and Terence Sanger. He leads the research data science program with CHOC, focusing on a wide breath of computational and data science research from the application of applied statistical learning on structured electronic medical records to the application of deep learning for computer vision and natural language processing in pediatric medicine. He has led deployment of various statistical and machine learning models in the electronic medical record (EMR) resulting in improved quality of care.

HONGXIA LU received the first master's degree in business analytics and project management from the University of Connecticut, the second master's degree in statistics from Michigan State University, and the Ph.D. degree in computational and data sciences from Chapman University, in 2022. She is a Data Scientist with the Data Analytics Team in Abacus Evaluation. Her expertise lies in using machine learning and deep learning algorithms to answer questions in the medical field, with a focus on natural language processing algorithms on unstructured medical notes and supervised and unsupervised learning algorithms on medical digital signal data.

YONGJUAN GUO received the degree in clinical medicine from Zhejiang University School of Medicine, in July 2001. She is a distinguished medical professional with an illustrious academic journey and extensive expertise in the field of clinical medicine, particularly cardiovascular medicine. She has consistently demonstrated a commitment to excellence in medical practice and research.

SHENGLIN LIU received the bachelor's degree from Zhongshan Medical University, in 1991.

He is a highly accomplished medical professional with a solid academic foundation and extensive experience in cardiovascular medicine. He has pursued a distinguished career, making significant contributions to clinical practice and research. He has held various roles, starting as a Resident Physician with Eastern Hospital and progressing to become an attending physician in cardiology. With expertise in functional examination and a focus on cardiovascular diseases, he is currently an Associate Chief Physician with the Electrocardiography Unit, Cardiovascular Department, Eastern Hospital. Throughout the years, he has been actively involved in research, contributing to numerous publications in esteemed medical journals. Notable works include investigations into acute myocardial infarction, the effects of thrombolysis on QT interval dispersion, and the impact of coronary artery lesions on QT interval dispersion.

HUIMIN CHU is a distinguished and accomplished cardiologist, holding significant positions and making impactful contributions to the field of cardiology. As a Chief Physician, a Professor, and the Doctoral Supervisor, he is the Director of the Heart Rhythm Center and the Deputy Director of the Heart Center. He is recognized for his pioneering work, being the founder of "Book, Heart, Sword, and Law." His leadership extends to various national committees and associations, emphasizing his influence in shaping cardiovascular care policies and practices. With extensive clinical expertise, he has played a pivotal role in the advancement of arrhythmia treatment in China. Notably, he is one of the founders of Green Electrophysiology, One-Stop Atrial Fibrillation Care, and Green Left Atrial Appendage Occlusion. He has conducted over 15,000 radiofrequency ablations and more than 1,200 left atrial appendage occlusions, as the first doctor in Ningbo to perform heart surgery abroad. His contributions extend to research, with over 20 SCI articles, five national guidelines, and leadership in three nationwide multicenter registry studies.

His editorial roles in prestigious journals and his recognition as the "Top Ten Clinical Innovator in Arrhythmia," in 2022 by China Doctor News underscore his significant impact on the field of cardiology.

BING YANG received the Ph.D. degree in internal medicine from Nanjing Medical University, in 2005.

He is an accomplished and highly regarded cardiologist with a diverse academic and professional background. He has held various leadership positions in prestigious medical institutions, including the current role as the Executive Deputy Director and the Director of cardiovascular internal medicine with Shanghai East Hospital. His impactful research is evident in his numerous publications, covering a wide range of topics in cardiovascular medicine. Notable works include the development of novel electrocardiographic criteria, the rationale for cardiac neuromodulation therapy, and studies on catheter ablation techniques for atrial fibrillation.

Dr. Yang actively contributes to the medical community and holding committee memberships and chairing positions in esteemed organizations, such as the Chinese Medical Association and the National Health Commission, where he serves as a Tutor for cardiac arrhythmia intervention training. Throughout his career, he has received notable recognition, including the China Top Doctor Awards, in 2018.

● ● ●